J Sol-Gel Sci Technol (2017) 83:467–477
DOI 10.1007/s10971-017-4413-0

Selective recovery of Au(III) from aqueous solutions by nano-silica grafted with 4-(aminomethyl) pyridine

Likang Fu[1,2,3] · Libo Zhang[1,2,3] · Shixing Wang[1,2,3] · Gengwei Zhang[1,2,3] · Jinhui Peng[1,2,3]

Received: 18 December 2016 / Accepted: 8 May 2017 / Published online: 20 May 2017

Abstract A new adsorbent was synthesized via functionalizing nano-silica with 4-(aminomethyl) pyridine for selective recovery of gold. The adsorbent was characterized by Fourier transform infrared spectroscopy, thermogravimetric analysis, X-ray photoelectron spectroscopy and transmission electron microscopy, and BET (surface area and porosimetry analyzer). The results indicated that the maximum adsorption capacity of Au(III) was 55.5 mg/g at pH 4.0 and room temperature. The adsorption reaction was fairly rapid and reached equilibrium within 30 min. The adsorption processes of Au(III) were fitted well to the Langmuir isotherm model and adsorption kinetics of Au(III) followed the pseudo-second-order rate equation. The adsorption mechanism lies on the chelation and ion exchange between gold ions and amines/hydroxyl groups. The adsorbent had good reusability after five cycles. Moreover, 4-(aminomethyl) pyridine-Silica nanoparticles has a good selectivity in the adsorption of Au(III) from the coexisting ions. Therefore, 4-(aminomethyl) pyridine functionalized nano-silica could be of great potential as new adsorbent for the selective recovery of Au(III) from industrial effluents and waste e-products.

Graphical Abstract

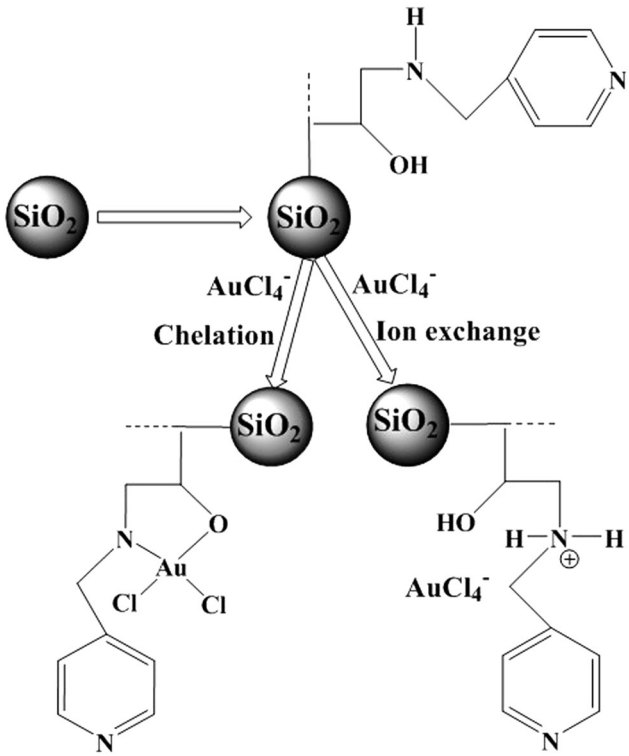

Keywords Selective recovery · Gold · Silica · Langmuir isotherm model · Adsorption kinetics

✉ Shixing Wang
wsxkm@sina.com

[1] State Key Laboratory of Complex Nonferrous Metal Resources Clean Utilization (Kunming University of Science and Technology), Kunming 650093 Yunnan, China

[2] National Local Joint Laboratory of Engineering Application of Microwave Energy and Equipment Technology, Kunming 650093 Yunnan, China

[3] Faculty of Metallurgical and Energy Engineering, Kunming University of Science and Technology, Kunming 650093 Yunnan, China

1 Introduction

With the excellent properties, gold has wide applications in various industrial fields such as electronic materials, catalysts, biomedicine, etc. [1–3]. However, the demand of gold is growing and gold resources are reducing. It is extremely important to remove and recycle gold from the primary and secondary resources.

Several methods have been employed to recycle gold from industry waste, for example, precipitation, electrolysis, solvent extraction, adsorption, and membrane technique [4–10]. Among these methods, adsorption is regarded as an efficient approach in both economy and technology, due to easy operating, suitable for low concentration of metal ions, low cost, and saving time. So there are a wide variety of adsorbents, such as resins [11–13], zeolite [14], molecular-imprinted biosorbent [15], chitosan resin [16], and magnetic particles [17, 18].

Recently, nano-materials have been developed as efficient adsorbents because of its excellent physiochemical performance that cannot be achieved by bulk materials [19]. As a nano-adsorbent, nano-silica has some unique superiority in the removal and recovery of metal ions [20], such as lead [21], copper [22], mercury [23], cadmium, and nickel [24].

In this study, 4-(aminomethyl) pyridine (AMPD) was modified on the surface of nano-silica for adsorption and recovery of Au(III). The new adsorbent was characterized by Fourier Transform infrared spectroscopy (FT-IR), thermo-gravimetric analysis (TGA), X-ray photoelectron spectroscopy (XPS), and transmission electron microscopy (TEM). The effect of pH values, initial Au(III) concentration and reaction time on the adsorption capacity of Au(III) was assessed. The isotherms and kinetics parameters of adsorption experiments were calculated. The reusability and adsorption mechanism of the adsorbent were investigated. In addition, selective adsorption of gold from dualistic solution was also studied.

2 Materials and methods

2.1 Materials

Silica nanoparticles (SNP, Hydrophilic-380, 99.8%), glycidyl methacrylate (97%), 3-Chloropropyltriethoxysilane (CPTS, 98%), AMPD 98%, and Chloroauric acid hydrate (HAuCl4·4H2O, 99.95%) were purchased from Aladdin Chemistry Co. Ltd, N,N-Dimethylformamide (DMF, 99.5%), Cuprous chloride (99.95%), 4,4-Bipyridine (98%), ethanol (99.8%), ammonia (99.5%), thiourea (99%), ZnCl2 (98%), PbCl2 (98%), MgCl2 (99%), CuCl2 (99.9%), and HNO3 (99.5%) were purchased from Tianjin Rgent Chemical Reagent Co. Ltd. The pH of the solution was adjusted with HCl (99.5%) and NaOH (99%).

2.2 Preparation of AMPD-SNP

The new adsorbent was prepared by grafting AMPD on the surface of SNP (Scheme 1). Firstly, the halogenated hydrocarbons (C–Cl) were grafted on the surface of SNP via silanization. We added 5.0 g of SNP, 15 mL of CPTS, 4 mL of ammonia, and 80 mL of ethanol (ratio was 1:20) into a 100 mL three-necked flask. The mixture was stirred and refluxed at 340 K for 24 h. After centrifuged, the solid was washed with ethanol for five times and then dried in a vacuum oven at 355 K for 6 h, defined as CPTS-SNP. Secondly, the epoxy groups were grafted on the CPTS-SNP via atom transfer radical addition polymerization [25]. CPTS-SNP (2 g) and glycidyl methacrylate (10 mL) were dissolved in 80 mL of DMF, 30 mg of CuCl and 90 mg of 4,4-Bipyridine were added as the catalyst. After stirred and refluxed under N_2 for 24 h at 345 K, the mixture was centrifuged and washed with DMF for five times, dried in a vacuum oven at 355 K for 6 h and obtained GMC-SNP. Finally, AMPD was grafted via ring opening reaction of epoxy groups. 1.65 g of GMC-SNP and 4 mL of AMPD were added into 80 mL of ethanol. After stirred and refluxed at 345 K for 24 h, the precipitate was centrifuged and washed with ethanol for five times, dried in a vacuum oven at 355 K for 6 h, and then we denoted it as AMPD-SNP.

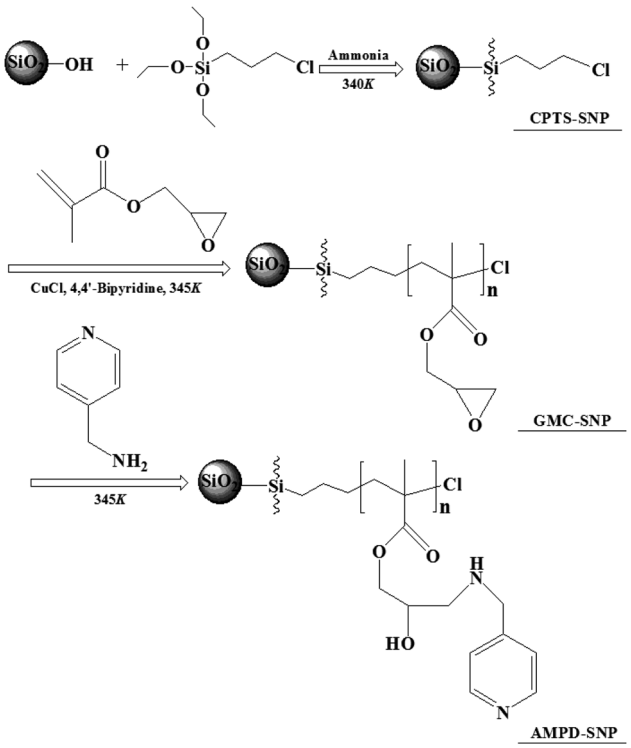

Scheme 1 Procedure for the preparation of AMPD-SNP

2.3 Batch adsorption experiment

The batch adsorption of Au(III) onto AMPD-SNP was carried out at room temperature. Twenty milligram of AMPD-SNP were added into 10 mL of aqueous solution containing a certain gold ions concentration. We shook it at 300 r.p.m., centrifuged the suspension at 8000 r.p.m. for 2 min. The remaining concentration of metal ions in the supernatant solution was determined by inductively coupled plasma optical emission spectrometry. The adsorption efficiency ($R\%$) and equilibrium adsorption capacity (q_e mg/g) of Au(III) were calculated by the following Eq. 1 and Eq. 2, respectively:

$$R = \frac{(C_0 - C_e)}{C_0} \times 100\% \tag{1}$$

$$q_e = \frac{(C_0 - C_e)}{m} V \tag{2}$$

where C_0 (mg/L) and C_e (mg/L) are the initial and remaining concentrations of Au(III) in the testing solution, respectively. V (L) is the volume of the testing solution and m (mg) is the weight of AMPD-SNP.

2.4 Characterization

FT-IR was obtained by a Nicolet iS50 FT-IR spectrophotometer (Thermo Nicolet, USA) with a resolution of 4 cm^{-1}. XPS was tested with a PHI5000 Versaprobe-II (Physical Electronics, Inc., Chanhassen, MN, USA) using 200 W Mg radiations. TEM (JEM-3200) was used to characterize the size and morphology of nano-silica. TGA measurements were carried out on PerkinElmer TGA-7 (America) thermogravimetric analyzer at a heating rate of 20℃/min. BET (surface area and porosimetry analyzer) specific surface area was tested by Micromeritics, ASAP 2020 surface and pore analyzer. The concentrations of Au (III), Pb(II), Cu(II), Zn(II), and Mg(II) were determined with inductively coupled plasma optical emission spectrometer (ICP-OES, LEEMAN prodigy 7, America).

2.5 Adsorption isotherms and kinetic studies

Adsorption isotherms and kinetic were studied by using different models. The Freundlich isotherm model has a wide range of applicability and a simple formulation. It has high practical value in some fields and is applied to adsorption of gas or solute on solid surface. The linear form of the Freundlich isotherm is given as Eq. 3:

$$\lg q_e = \lg K_F + \frac{1}{n} \lg C_e \tag{3}$$

where q_e (mg/g) is the adsorption capacity of Au(III) at equilibrium, C_e (mg/L) is the equilibrium concentration of Au(III) in solution, K_F is a constant relevant to the adsorption capacity and n is the constant indicative of the intensity of the adsorption.

The Langmuir adsorption process is monolayer adsorption, and the linear form of the Langmuir isotherm is expressed as Eq. 4:

$$\frac{1}{q_e} = \frac{1}{q_m} + \frac{1}{K_L q_m} \bullet \frac{1}{C_e} \tag{4}$$

where q_m (mg/g) is the maximum adsorption capacity and K_L is the Langmuir binding constant relevant to energy of adsorption.

In the Temkin isothermal condition, the heat of adsorption is linearly reduced between the adsorbate and the adsorbent. The linear form of the Temkin isotherm is written as Eq. 5:

$$q_e = B_T ln\, K_T + B_T ln\, C_e \tag{5}$$

where B_T is relevant to the heat of adsorption, K_T is the equilibrium binding constant (L/g).

The kinetics of Au(III) was analyzed using pseudo-first-order, pseudo-second-order and intraparticle diffusion kinetic models. Those can be expressed as the Eqs 6, 7, and 8, respectively:

$$ln(q_e - q_t) = ln\, q_e - K_1 t \tag{6}$$

$$\frac{t}{q_t} = \frac{t}{q_e} + \frac{1}{K_2 {q_e}^2} \tag{7}$$

$$q_t = K_i t^{1/2} + C \tag{8}$$

where q_t (mg/g) and q_e (mg/g) were the amounts of Au(III) adsorbed per gram adsorbent at time t and at equilibrium, respectively. K_1 and K_2 (g/mg·min) were the rate constants of the pseudo-first-order and pseudo-second-order model. K_i (mg/g·$min^{1/2}$) was the rate constant of intraparticle diffusion model, C was an indicator for expressing the boundary layer thickness.

3 Result and discussion

3.1 Characterization of the sorbents

The FT-IR spectra of the nano-silica modified with organics were shown in Fig. 1. The peaks at 1102 and 3425 cm^{-1} belong to Si–O–Si and O–H stretching vibration (Fig. 1a) [26]. When CPTS was grafted on the surface of nano-silica, the peaks at 800, 1102, 2868, and 3425 cm^{-1} belong to C–Cl, Si–O–Si, $-CH_2$, and O–H stretching vibration (Fig. 1b) [27]. After modified by glycidyl methacrylate, the vibration peak of epoxy group and C–C=O were locating at 1250 and 1680 cm^{-1} (Fig. 1c) [27, 28]. The new vibration peaks of C–OH, pyridine ring and –NH appeared in 1150,

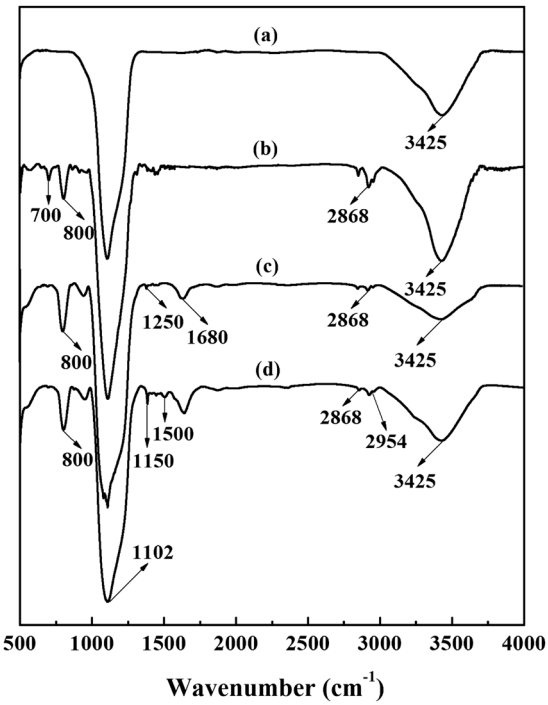

Fig. 1 FT-IR spectra of SNP (**a**), CPTS-SNP (**b**), GMC-SNP (**c**), and AMPD-SNP (**d**)

1500, and 2954 cm^{-1} after modified by AMPD, respectively (Fig. 1d) [28].

Figure 2 showed the TGA of SNP, CPTS-SNP, GMC-SNP, and AMPD-SNP. The mass losses of them were 8, 11, 15, and 22% in the temperature range of 20 to 1000°C, respectively. In the TGA, mass loss was caused by the decomposition of organic matter and the evaporation of water. From Fig. 2, we could determine that the amount of the CPTS, the glycidyl methacrylate and the AMPD were 3, 4, and 7%, respectively.

BET surface area of CPTS-SNP is 120 m2/g, and the calculated density of the CPTS groups is $4.5 \times 1018\ m^{-2}$. This indicated that CPTS has been successfully grafted onto the surface of nano-silica.

XPS is an effective means of analysis for validating the elemental composition of a compound. Figure 3 is the survey spectra for these samples. The characteristic peaks of Si2p, Si2s, O1s, and C1s were observed. After modified by AMPD, the nitrogen peak at 398.2 eV was observed in the spectrum. The C1s peaks of the modified nano-silica were shown in Fig. 4. The C1s peaks of CPTS-SNP appeared in 284.6 and 287.5 eV, due to the C–C and C–Cl bonds (Fig. 4a). In Fig. 4b, two new bonds of GMC-SNP were generated. The peaks of C–O–C and O=C–O bonds were locating at 285.4 and 287.9 eV, respectively. After modified with AMPD, the epoxy bond (C–O–C) was opened and three new bonds (C–O, C–N, and C=N) were generated (Fig. 4c). The C1s peaks of AMPD-SNP was divided into

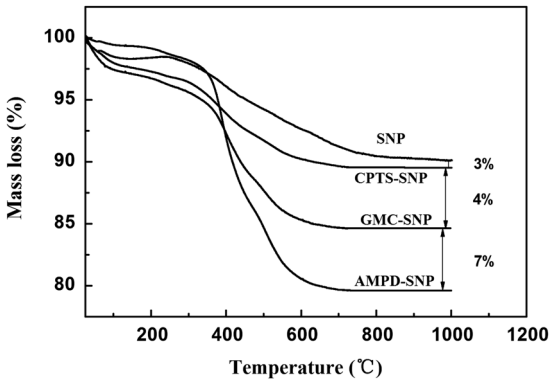

Fig. 2 TGA dates of SNP, CPTS-SNP, GMC-SNP, and AMPD-SNP

five species (C–C, C–O, C–N, C=N, O=C–O), locating at 284.6, 285.2, 285.8, 287.7, and 287.9 eV, respectively.

In order to explore the morphology and size, TEM is widely used in various fields, including material science and geological minerals [29, 30]. As shown in Fig. 5, the particles size of SNP and AMPD-SNP were both 22.3 ± 5 nm. The results of TEM showed the morphology and size of SNP and AMPD-SNP were not much changed.

3.2 Effect of pH

As one of the important factors affecting the adsorption of metal ions, the pH value of the solution can promote the depolymerization of the functional groups of the sorbent and adjust the electrostatic adsorption or complexation reaction [31]. For preventing formation of gold hydroxide precipitates when pH is too high, we investigated the effect of pH on the adsorption of Au(III) in the range of 0.5 to 8.0. 20 mg of AMPD-SNP was added to 10 mL of gold ion solution (100 mg/L). We shook it for 60 min at room temperature and got the remaining concentration of Au(III) by centrifugation. As shown in Fig. 6, the adsorption efficiency has been continuously improved, and then decreased with the increase of pH value when pH was greater than 4.0. At low pH values, the competition adsorption between Cl^- and $AuCl4^-$ affected the adsorption of Au(III) by AMPD-SNP [32]. With the increasing of pH value, the hydroxo-containing gold complex such as AuCl3(OH)– emerged in solution, resulting in a decrease of electrostatic attractions between the negatively charged Au(III) anions and the positively charged adsorption sites of AMPD-SNP [33, 34]. Thus the optimum pH is 4.0.

3.3 Effect of initial Au(III) concentration and adsorption isotherms

In order to study the effect of the initial concentration of Au (III) on the adsorption capacity, we added 20 mg of AMPD-

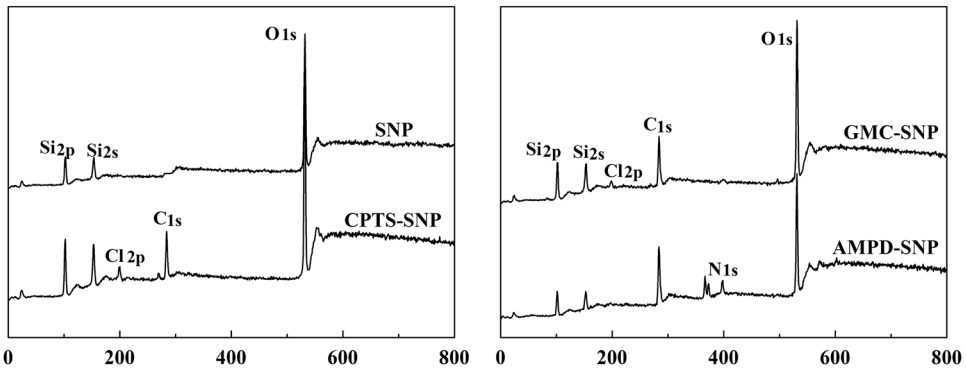

Fig. 3 XPS spectra of SNP, CPTS-SNP, GMC-SNP, and AMPD-SNP

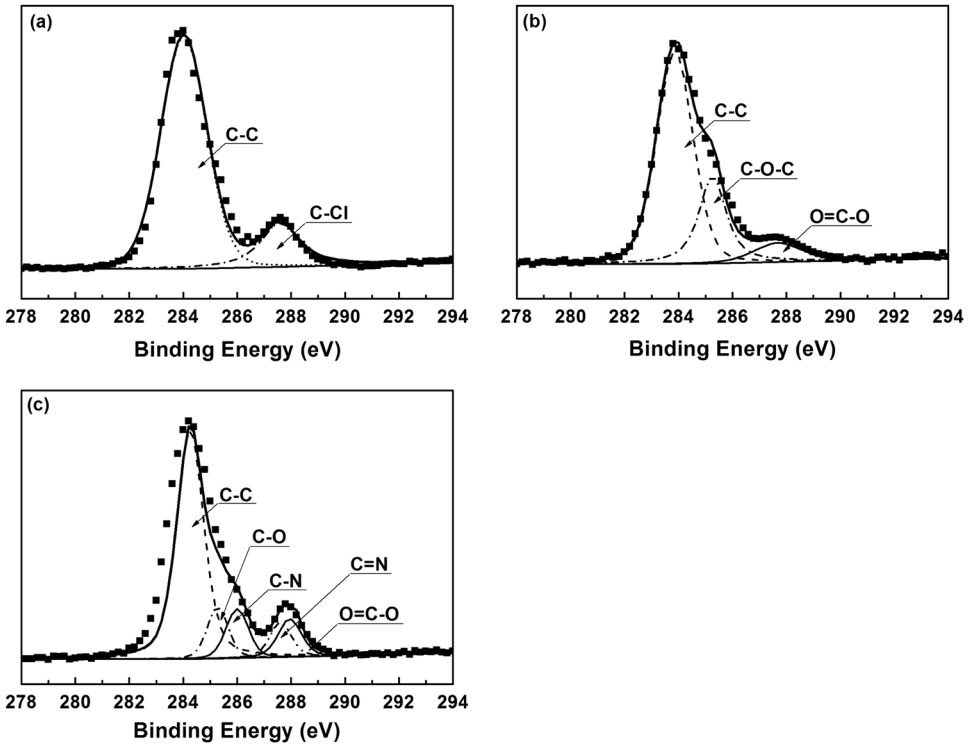

Fig. 4 C1s of CPTS-SNP (**a**), GMC-SNP (**b**), and AMPD-SNP (**c**)

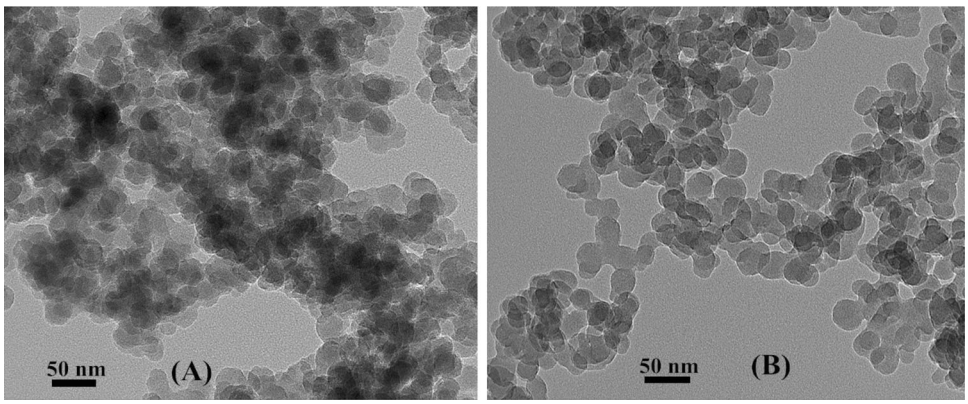

Fig. 5 TEM images of SNP (**a**) and AMPD-SNP (**b**)

SNP to 10 mL of gold ion solution containing the following concentrations (80, 90, 100, 110, 120, 200, 300, 400, 500, and 600 mg/L) at pH 4.0. As shown in Fig. 7, the adsorption capacity of Au(III) increased with the increase of the Au(III) concentration. The maximum adsorption capacity of Au(III) is 55.5 mg/g, because there is a strong interaction between

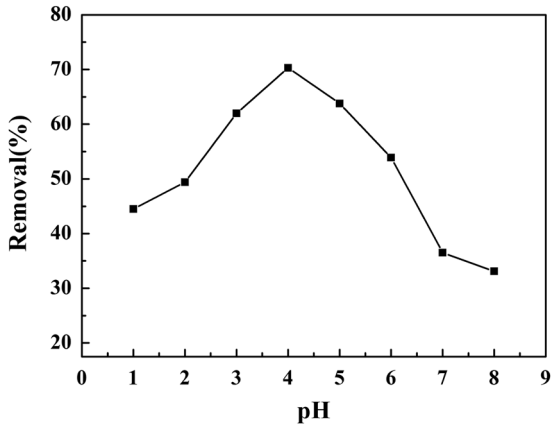

Fig. 6 Effect of solution pH on the removal rate of Au(III)

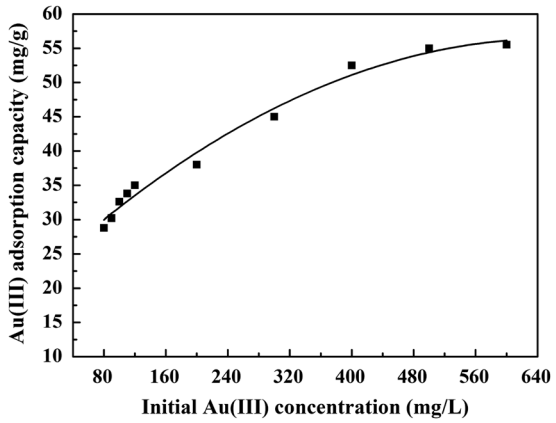

Fig. 7 Effect of initial Au(III) concentration on the adsorption of Au (III)

the metal ions with the nitrogen lone-pair on the surface of AMPD-SNP adsorbent [35].

The adsorption isotherm shows how the adsorbent interacts with the gold ion, and how the adsorption capacity varies with the adsorption concentration [22]. We presented the adsorption capacity of Au(III) and equilibrium concentration by Freundlich, Langmuir, and Temkin isotherm models at pH 4.0 and room temperature. [36, 37]

From Fig. 8a, $\lg C_e$ vs. $\lg q_e$ was drew by the values of Freundlich model. K_F, R^2 and n were presented in Table 1. The R^2 coefficient is only 0.9025 and the n value is 2.2999, suggesting these data do not conform to the Freundlich isotherm model.

q_m and K_L were gained from Fig. 8b and shown in Table 1. The correlation coefficient (R^2) of Langmuir isotherm model was 0.9992, indicating the adsorption of Au (III) were fitted particularly well with the Langmuir isotherm model. The adsorption mechanism was verified by the high K_L.

As shown in Fig. 8c, the values of Temkin model were used to draw $\ln C_e$ vs. q_e, K_T and B_T had been calculated and presented in Table 1. The correlation coefficient (R^2) was only 0.9745, thus the experimental data did not follow the Temkin isothermal model.

The maximum adsorption capacity was 55.5 mg/g and monolayer adsorption happened on the nano-silica grafted with AMPD. The AMPD-SNP is an efficient sorbent. The adsorption capacity of AMPD-SNP and other results reported in literature were listed in Table 2. So the AMPD-SNP sorbent shows great potential in the field of adsorption and recycling of Au(III).

3.4 Effect of reaction time and adsorption kinetics

In order to study the effect of reaction time on the adsorption by AMPD-SNP, we added 20 mg of AMPD-SNP to 10 mL of Au(III) solution (100 mg/L of initial concentration) at pH 4.0 and room temperature. As shown in Fig. 9, the adsorption rate of Au(III) was fast during the first 10 min. It took only 30 min to reach adsorption equilibrium. Chelation and ion exchange were the main mechanisms in the adsorption process.

For further study the adsorption mechanism, the Lagergren pseudo-first order, pseudo-second order, and intraparticle diffusion kinetic models were used to describe the adsorption kinetics of Au(III).

Kinetics parameters K and correlation coefficients R^2 were calculated and gathered in Table 3. The R^2 of the pseudo-first-order model was 0.9216, so it is difficult to fulfill the adsorption principle of this experiment (Fig. 10a). According to the intraparticle diffusion model, if the line plotted by q_t vs. $t^{1/2}$ is straight and through the origin, the intraparticle diffusion is controlling step [38]. As shown in Fig. 10c, we found that the fitted straight lines did not pass through the origin and the R^2 was only 0.9604. Thus, the intraparticle diffusion was not suitable for describing adsorption kinetics. From Fig. 10b, the correlation coefficients (R^2) was 0.9998, indicating that the pseudo-second-order model was fitting well the adsorption kinetics of Au (III) using AMPD-SNP.

3.5 Desorption and reusability of AMPD-SNP

100 mg of AMPD-SNP was added to 50 mL of Au(III) solution (the initial concentration was 100 mg/L). After shook for 60 min, the mixed solution was centrifuged, and then we took the supernatant. An eluent consisting of thiourea (0.1 M) and HNO3 (3wt%) was used to retreat the AMPD-SNP adsorbent. Lastly, we regained the AMPD-SNP sorbent. The change of the adsorption efficiency was described in Fig. 11. After five successive cycles, the adsorption efficiency was reduced slightly from 71.25 to 69.01%. This proved that AMPD-SNP had good stability and high efficiency for the repeated use after five cycles.

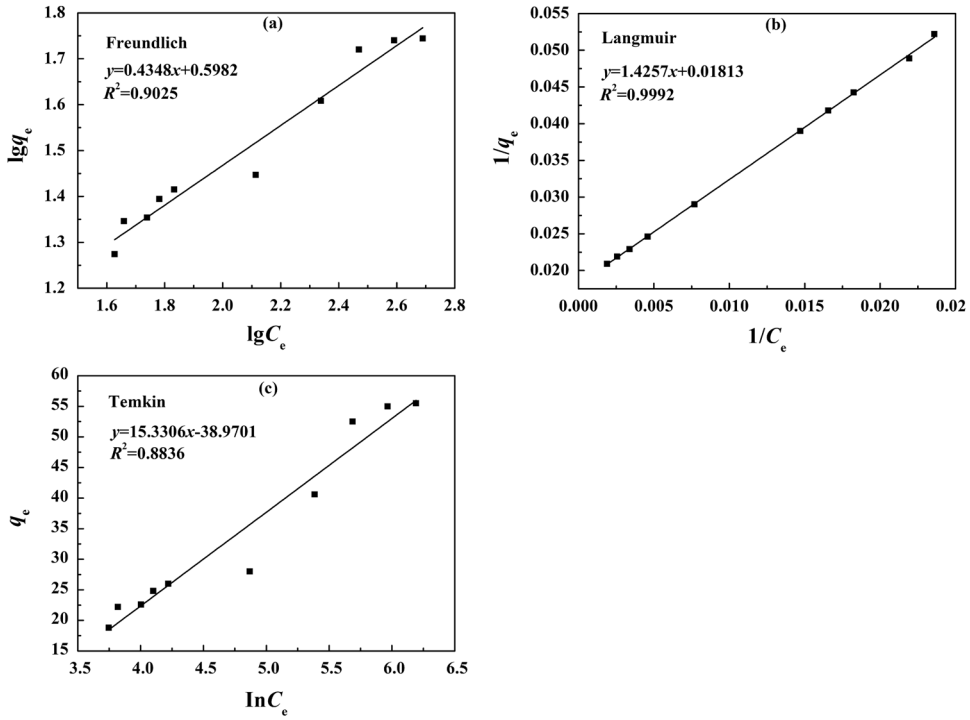

Fig. 8 Adsorption isotherms of Au(III) onto AMPD-SNP, Freundlich (**a**), Langmuir (**b**), and Temkin (**c**)

Table 1 Isotherm parameters for the adsorption of Au(III) by the AMPD-SNP at 298 K

Isotherm model	Parameter	Value
Freundlich	K_F [(mg g^{-1})/(mg L^{-1})$^{1/n}$]	3.9646
	n	2.2999
	R^2	0.9025
	q_m(mg/g)	55.2
Langmuir	K_L(L/g)	0.0127
	R^2	0.9992
	K_T (L/g)	0.0787
Temkin	B_T(J/mol)	15.331
	R^2	0.8836

Table 2 Comparison of adsorption capacity of gold with sorbents reported in literature

Sorbent	qm(mg/g)	References
SiG-Schiff bases	0.2	[36]
Heated-immobilized *C. vulgaris*	10.34	[37]
Heated rice husk	28.22	[37]
Activated carbon	35.88	[37]
AMPD-SNP	55.5	This work

3.6 Adsorption mechanism of Au(III) onto AMPD-SNP

To clarify the adsorption mechanism of Au(III) onto AMPD-SNP, XPS of the adsorbent before and after the

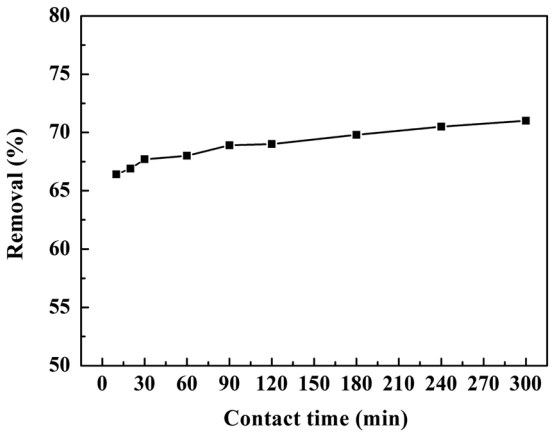

Fig. 9 Effect of contact time on the removal rate of Au(III)

Table 3 Kinetics parameters for the adsorption of Au(III) by AMPDT-SNP

Kinetic models	Parameter	Value
Pseudo-first-order	K_1(g/mg·min)	0.0088
	R^2	0.9216
Pseudo-second-order	K_2(g/mg·min)	0.0128
	R^2	0.9998
	K_i (mg/g·min$^{1/2}$)	0.03234
Intraparticle diffusion	C	22.8175
	R^2	0.9604

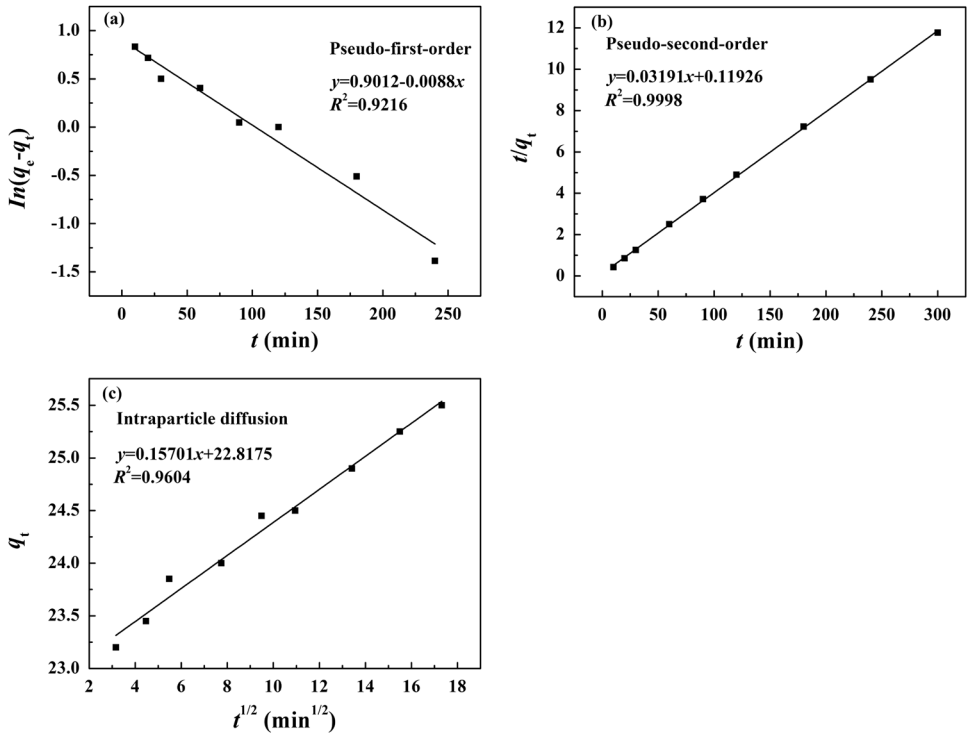

Fig. 10 Adsorption kinetics of Au(III) onto AMPD-SNP, Pseudo-first-order (**a**), pseudo-second-order (**b**), and intraparticle diffusion models (**c**)

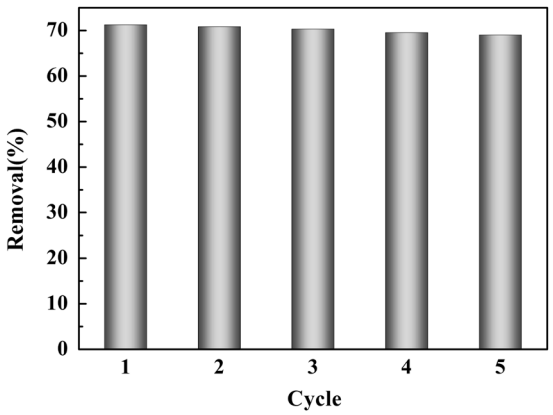

Fig. 11 Reusability of adsorbent for removal of Au(III) after five successive cycles of adsorption/desorption

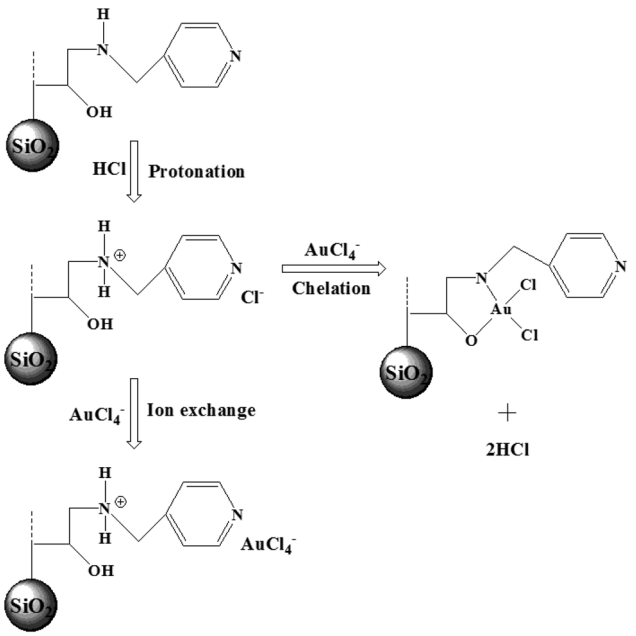

Scheme 2 Mechanism of the adsorption of Au(III) onto AMPD-SNP

adsorption of Au(III) were conducted. From Fig. 12a, the N1s spectrum of AMPD-SNP could be fitted into three peaks (C=N, –NH/–NH_2, –NH_2^+), locating at 398.5, 399.4, and 400.5 eV, respectively. After adsorbed the gold ions, the binding energy of some –NH/–NH_2 groups reached at 400.4 eV, suggesting that the amino group has bound to Au(III) ions by chelation. At the same time, the peak of –NH_2^+ was broadened, indicating that many amino groups had been protonated (Fig. 12b). This was the premise of ion exchange with gold ions. As shown in Fig. 12c, the binding energy of Au4f was roughly locating at 83.0 and 89.1 eV in AMPD-SNP-Au. It was much lower than that in Au(III), showing that Au(III) had accepted electrons during adsorption process [39]. From the above results, we verified that the adsorption mechanism was the chelation and ion exchange reaction between Au(III) and amines/hydroxyl groups (Scheme 2). On one hand, the amines and hydroxyl groups of the surface of adsorbent reacted with $AuCl_4^-$ by direct chelation, on the other hand, the amino group was protonated by hydrochloric acid at first, and then adsorbed gold ions by ion exchange

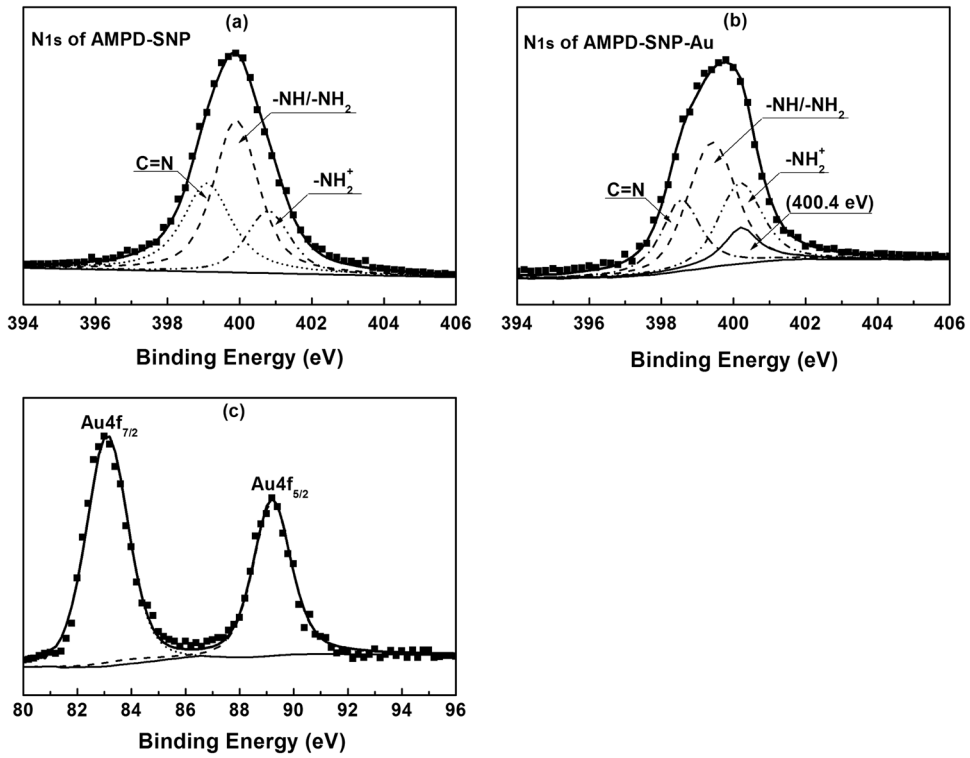

Fig. 12 N1s of AMPD-SNP (**a**) and AMPD-SNP-Au (**b**), and Au4f of AMPD-SNP-Au (**c**)

Table 4 Selective adsorption of Au(III) form the coexisting metal ions by AMPD-SNP

Coexisting ions	Au(III)	Au(III) + Pb(II)		Au(III) + Cu(II)		Au(III) + Zn(II)		Au(III) + Mg(II)	
		Au(III)	Pb(II)	Au(III)	Cu(II)	Au(III)	Zn(II)	Au(III)	Mg(II)
Removal rate (*R* %)	72.6	72.4	7.12	71.2	16.3	70.0	14.4	70.3	13.4

[39]. Sun et al. have also suggested that the mechanism of adsorption of gold ions is the reaction between gold ions and amines and hydroxyl groups [40].

3.7 Selective adsorption of Au(III) onto AMPD-SNP

Selective adsorption of Au(III) from dualistic solution by the AMPD-SNP was studied at pH 4.0 and with other conditions fixed. The solution contained Pb(II), Cu(II), Zn (II), and Mg(II), respectively. Twenty milligram of AMPD-SNP was added into 10 mL of dualistic solutions containing Au(III) (100 mg/L) and coexisting metal ions (100 mg/L), and then shook it for 60 min at room temperature. After centrifugation, the remaining concentrations of gold ions and coexisting metal ions were detected. From Table 4, we found that the adsorption efficiency of the coexisting ions were much less than Au(III). The reason was that the binding ability between Au(III) and amino were much stronger than other metal ions,. The results indicated that Au(III) can be selectively adsorbed by AMPD-SNP from the mixed solution.

4 Conclusions

In this study, a new adsorbent for Au(III) was successfully synthesized by grafting with AMPD on nano-materials. FT-IR, TGA, XPS, TEM, and BET were used to characterize the adsorbent. The effects of solution pH, contact time, and initial Au(III) concentration on the adsorption of Au(III) have been studied. The optimum pH for the recovery of Au (III) was 4.0. The maximum uptake of Au(III) was 55.5 mg/g at pH 4.0 and room temperature. The adsorption equilibrium was reached at 30 min and the adsorption mechanism was the complexation and ion exchange reaction between Au(III) and amino functional groups. The adsorption of Au(III) by AMPD-SNP fitted well with the Langmuir isotherm model and also followed the pseudo second-order kinetics. AMPD-SNP had excellent reusability after several cycles and exhibited high selectivity to Au(III). Thus AMPD functionalized SNPs could be of great potential as novel adsorbent for the selective recovery of Au(III) from wastewater.

Acknowledgements The authors are grateful for the financial support from the National Natural Science Foundation (No. 51464024 and 51664037).

Compliance with ethical standards

Conflict of interest The authors declare that they have no competing interests.

References

1. Das N (2010) Recovery of precious metals through biosorption-a review. Hydrometallurgy 103:180–189
2. Syed S (2012) Recovery of gold from secondary sources - a review. Hydrometallurgy 115:30–51
3. Skrabalak SE, Chen J, Au L, Lu X, Li X, Xia Y (2007) Gold Nanocages for biomedical applications. Adv Mater 20:3177–3184
4. Ma G, Yan WF, Chen J, Yan CH, Shi N, Wu JG, Xu GX (2000) Progress in gold solvent extraction. Prog Nat Sci 10:881–886
5. Fan RY, Xie F, Guan XL, Zhang QL, Luo ZR (2014) Selective adsorption and recovery of Au(III) from three kinds of acidic systems by persimmon residual based bio-sorbent: a method for gold recycling from e-wastes. Bioresour Technol 163:167–171
6. Sun CM, Zhang GH, Wang CH, Qu RJ, Zhang Y, Gu QY (2011) A resin with high adsorption selectivity for Au(III): preparation, characterization and adsorption properties. Chem Eng J 172:713–720
7. Pang SK, Yung KC (2014) Prerequisites for achieving gold adsorption by multiwalled carbon nanotubes in gold recovery. Chem Eng Sci 107:58–65
8. Soylak M, Cay RS (2007) Separation/preconcentration of silver(I) and lead(II) in environmental samples on cellulose nitrate membrane filter prior to their flame atomic absorption spectrometric determinations. J Hazard Mater 146:142–147
9. Tang B, Yu G, Fang J, Shi T (2010) Recovery of high-purity silver directly from dilute effluents by an emulsion liquid membrane-crystallization process. J Hazard Mater 177:377–383
10. Rofouei MK, Payehghadr M, Shamsipur M, Ahmadalinezhad A (2009) Solid phase extraction of ultra traces silver(I) using octadecyl silica membrane disks modified by 1,3-bis (2-cyanobenzene) triazene (CBT) ligand prior to determination by flame atomic absorption. J Hazard Mater 168:1184–1187
11. Atia A (2005) Adsorption of silver(I) and gold(III) on resins derived from bisthiourea and application to retrieval of silver ions from processed photo films. Hydrometallurgy 80:98–106
12. Donia AM, Atia A, El-Boraey HA, Mabrouk DH (2006) Adsorption of Ag(I) on glycidyl methacrylate/N,N0-methylene bis-acrylamide chelating resins with embedded iron oxide. Sep Purif Technol 48:281–287
13. Lam YL, Yang D, Chan CY, Chan KY, Toy PH (2009) Use of water-compatible polystyrene-polyglycidol resins for the separation and recovery of dissolved precious metal salts. Ind Eng Chem Res 48:4975–4979
14. Akgul M, Karabakan A, Acar O, Yurum Y (2006) Removal of silver(I) from aqueous solutions with clinoptilolite. Micropor Mesopor Mater 94:99–104
15. Huo HY, Su HJ, Tan TW (2009) Adsorption of Ag^{+} by a surface molecular- imprinted biosorbent. Chem Eng J 150:139–144
16. Donia AM, Atia A, Elwakeel KZ (2007) Recovery of gold(III) and silver(I) on a chemically modified chitosan with magnetic properties. Hydrometallurgy 87:197–206
17. Kraus A, Jainae K, Unob F, Sukpirom N (2009) Synthesis of MPTS-modified cobalt ferrite nanoparticles and their adsorption properties towards Au(III). J Colloid Interf Sci 338:359–365
18. Jainae K, Sanuwong K, Nuangjamnong J, Sukpirom N, Unob F (2010) Extraction and recovery of precious metal ions in wastewater by polystyrene-coated magnetic particles functionalized with 2-(3-(2-aminoethylthio)propylthio)ethanamine. Chem Eng J 160:586–593
19. Nguyen-Phan TD, Pham HD, Kim S, Oh ES, Kim EJ, Shin EW (2010) Surfactant removal from mesoporous TiO_2 nanocrystals by supercritical CO_2 fluid extraction. J Ind Eng Chem 16: 823–828
20. Pourreza N, Rastegarzadeh S, Larki A (2014) Nano-TiO_2 modified with 2-mercaptobenzimidazole as an efficient adsorbent for removal of Ag(I) from aqueous solutions. J Ind Eng Chem 20:127–132
21. Li X, Wang Z, Li Q, Ma J, Zhu M (2015) Preparation, characterization, and application of mesoporous silica-grafted graphene oxide for highly selective lead adsorption. Chem Eng J 273:630–637
22. Ali L, Ibrahim W, Sulaiman A, Kamboh MA, Sanagi MM (2016) New chrysin-functionalized silica-core shell magnetic nanoparticles for the magnetic solid phase extraction of copper ions from water samples. Talanta 148:191–199
23. He C, Ren L, Zhu W, Xu Y, Qian X (2015) Removal of mercury from aqueous solution using mesoporous silica nanoparticles modified with polyamide receptor. J Colloid Interf Sci 458:229–234
24. Xie F, Lin X, Wu X, Xie Z (2008) Solid phase extraction of lead (II), copper(II), cadmium(II) and nickel(II) using gallic acid-modified silica gel prior to determination by flame atomic absorption spectrometry. Talanta 74:836–843
25. Shiho H, Desimone JM (2001) Dispersion polymerization of Glycidyl methacrylate in supercritical carbon dioxide. Macromolecules 34:1198–1203
26. Sharma S, Wu CM, Koodali RT, Rajesh N (2016) An ionic liquid-mesoporous silica blend as a novel adsorbent for the adsorption and recovery of palladium ions, and its applications in continuous flow study and as an industrial catalyst. RSC Adv 6:26668–26678
27. Kima HC, Yub MJ (2005) Characterization of natural organic matter in conventional water treatment processes for selection of treatment processes focused on DBPs control. Water Res 39 (19):4779–4789
28. Zhang LB, Liu YH, Wang SX, Liu BG, Peng JH (2015) Selective removal of cationic dyes from aqueous solutions by an activated carbon-based multicarboxyl adsorbent. RSC Adv 5:99618–99626
29. Yang J, Duan X, Guo W, Li D, Zhang H, Zheng W (2014) Electrochemical performances investigation of NiS/rGO composite as electrode material for supercapacitors. Nano Energy 5:74–81
30. Ribeiro J, Taffarel SR, Sampaio CH, Flores D, Silva LF (2013) Mineral speciation and fate of some hazardous contaminants in coal waste pile from anthracite mining in Portugal. Int J Coal Geol 109-110:15–23
31. Manzoori JL, Amjadi M, Hallaj T (2009) Preconcentration of trace cadmium and manganese using 1-(2-pyridylazo)-2-naphthol-modified TiO_2 nanoparticles and their determination by flame atomic absorption spectrometry. Int J Environ Anal Chem 89:749–758
32. Li X, Zhang CC, Zhao R, Lu XF, Xu XR, Jia XT, Wang C, Li LJ (2013) Efficient adsorption of gold ions from aqueous systems with thioamide-group chelating nanofiber membranes. Chem Eng J 229:420–428
33. He ZW, He LH, Yang J, Lü QF (2013) Removal and recovery of Au(III) from aqueous solution using a low-cost lignin-based biosorbent. Ind Eng Chem Res 52:4103–4108

34. Qu R, Sun C, Wang M, Ji C, Xu Q, Zhang Y, Wang C, Chen H, Yin P (2009) Adsorption of Au(III) from aqueous solution using cotton fiber/chitosan composite adsorbents. Hydrometallurgy 100:65–71
35. Türkmen D, Yılmaz E, Öztürk N, Akgöl S, Denizli A (2009) Poly (hydroxyethyl methacrylate) nanobeads containing imidazole groups for removal of Cu(II) ions. A Mater Sci Eng C 29:2072–2078
36. Petrova P, Karadjova I, Chochkova M, Dakova I (2015) Solid phase extraction of Au(III) using silica gel modified with 4-aminoantipyrine schiff bases. Chem: Bulgarian J Sci Edu 24:441–448
37. Nakbanpote W, Thiravetyan P, Kalambaheti C (2002) Comparison of gold adsorption by Chlorella vulgaris, rice husk and activated carbon. Miner Eng 15:549–552
38. Hou H, Yu D, Hu G (2015) Preparation and properties of ion-imprinted hollow particles for the selective adsorption of silver ions. Langmuir 31:1376–1384
39. Dong Z, Liu JZ, Yuan WJ, Yi YP, Zhao L (2016) Recovery of Au (III) by radiation synthesized aminomethyl pyridine functionalized adsorbents based on cellulose. Chem Eng J 283:504–513
40. Sun CM, Zhang GH, Wang CH, Qu RJ, Zhang Y, Gu QY (2011) A resin with high adsorption selectivity for Au (III): preparation, characterization and adsorption properties. Chem Eng J 172:713–720